

Physical parameters and multiplicity of five southern close eclipsing binaries^{★,★★}

T. Szalai¹, L. L. Kiss^{2,3}, Sz. Mészáros^{1,4}, J. Vinkó¹, and Sz. Csizmadia⁵

¹ Department of Optics and Quantum Electronics, University of Szeged, Hungary

² School of Physics A28, University of Sydney, NSW 2006, Australia
e-mail: l.kiss@physics.usyd.edu.au

³ Department of Experimental Physics, University of Szeged, Hungary

⁴ Harvard-Smithsonian Center for Astrophysics, Cambridge, MA, USA

⁵ Konkoly Observatory of the Hungarian Academy of Sciences, Budapest, Hungary

Received 19 November 2006 / Accepted 2 January 2007

ABSTRACT

Aims. We detected tertiary components of close binaries from spectroscopy and light curve modelling, investigated the light-travel time effect and the possibility of magnetic activity cycles, measured mass ratios for unstudied systems, and derived absolute parameters.

Methods. We carried out new photometric and spectroscopic observations of five bright ($\langle V \rangle < 10.5$ mag) close eclipsing binaries, predominantly in the southern skies. We obtained full Johnson *BV* light curves, which were modelled with the Wilson-Devinney code. Radial velocities were measured with the cross-correlation method using IAU radial velocity standards as spectral templates. Period changes were studied with the O–C method, utilising published epochs of minimum light (XY Leo) and ASAS photometry (VZ Lib).

Results. For three objects (DX Tuc, QY Hya, V870 Ara), absolute parameters have been determined for the first time. We spectroscopically detected the tertiary components in XY Leo and VZ Lib and discovered one in QY Hya. For XY Leo we updated the light-time effect parameters and detected a secondary periodicity of about 5100 d in the O–C diagram that may hint at the existence of short-period magnetic cycles. A combination of recent photometric data shows that the orbital period of the tertiary star in VZ Lib is likely to be over 1500 d. QY Hya is a semi-detached X-ray active binary in a triple system with K and M-type components, while V870 Ara is a contact binary with the third smallest spectroscopic mass ratio for a W UMa star to date ($q = 0.082 \pm 0.030$). Being close to the theoretical minimum for contact binaries, this small mass ratio suggests that V870 Ara has the potential of constraining evolutionary scenarios of binary mergers. The inferred distances to these systems are compatible with the Hipparcos parallaxes.

Key words. stars: binaries: close – stars: binaries: eclipsing – stars: binaries: spectroscopic – stars: binaries: general

1. Introduction

Modelling variations of close eclipsing binaries is a powerful method for determining fundamental physical parameters of stars. This is because the observed brightness, colour, and radial velocity changes give strong constraints on the geometric configuration of a given system. W UMa-type stars are low-mass eclipsing contact binaries with orbital periods less than 1 day, showing continuous light variations. The components fill their Roche lobes so that the strongly distorted stars touch each other at the inner Lagrangian point. These systems have long been known as the most numerous of all stars, with roughly one W UMa binary per 500 ordinary dwarf stars (Rucinski 2002a), which is one of the reasons why many of them, including bright southern ones, are left unstudied until now. In particular, measuring radial velocities has been a tedious task with very slow progress. For instance, Bilir et al. (2005) noted that among the 751 recorded W UMa binaries in the recently revised fourth

edition of the General Catalog of Variable Stars, only 129 systems were found to have radial velocities, mostly northern ones. Very recently, Rucinski & Duerbeck (2006) and Duerbeck & Rucinski (2007) published radial velocities for 23 predominantly southern close binaries, but apart from that, there is basically no dedicated program for obtaining new data in the south. There are several important problems related to the formation, internal structure, and evolution of these systems, like the kinematics (e.g. Bilir et al. 2005), energy transfer between the components (Csizmadia & Klagyivik 2004, and references therein), magnetic activity and its cyclic nature (Borkovits et al. 2005), and the frequency of additional components of W UMa stars (Pribulla & Rucinski 2006, and references therein), all in need of more extensive data. The last is particularly important, because it is the angular momentum transfer in hierarchic triple systems that can lead to such close binary systems as W UMa-type stars, so one can even hypothesize that *all* contact binaries reside in triple or multiple systems (Pribulla & Rucinski 2006; D’Angelo et al. 2006). Testing this hypothesis is important, because angular momentum evolution, in which magnetic braking was shown to be a key factor in explaining the observed properties of contact binaries (Mochnacki 1981; Stepień 1995), can be strongly affected by the presence of a third body (Eggleton & Kiseleva-Eggleton 2001). In a wide range of initial conditions, an originally

* Based on observations made at the Siding Spring Observatory, Australia.

** Light curves and radial velocity data are only available in electronic form at the CDS via anonymous ftp to cdsarc.u-strasbg.fr (130.79.128.5) or via <http://cdsweb.u-strasbg.fr/cgi-bin/qcat?J/A+A/465/943>

detached binary can reach the contact phase, and this process can be altered by a tertiary star in the system (for a recent review see Eggleton 2006).

Late-type contact binary stars are known to be very active objects with stellar spots (Maceroni & van't Veer 1996) and X-ray radiation due to chromospheric activity (Stepien et al. 2001; Chen et al. 2006; Geske et al. 2006). These pieces of evidence can be interpreted by the Applegate-mechanism (Applegate 1992), which involves the interchange of magnetic and kinetic energy. An observable manifestation could be cyclic orbital period variation, which seems to be present in many contact binaries, although not necessarily caused by magnetic activity – for instance, the light-travel time effect due to a third body can also cause cyclic period change. Hence one must be cautious when interpreting the O–C diagrams in terms of cyclic changes. Observations so far seem to agree with the predictions of the orbital period–magnetic modulation period relation (Lanza & Rodonò 1999), and some of the studied systems were also analysed from this point of view.

Here we report on multicolour and radial velocity measurements of five close eclipsing binaries, of which three have never been studied before. In addition, the sample includes the well-studied quadruple system XY Leonis, which is one of the most fascinating cases of light-travel time effect in a periodic variable star (Gehlich et al. 1972; Yakut et al. 2003), and the triple system VZ Lib. Besides revealing new information on these two objects, the observations also allowed a comparison of our results with previous studies.

2. Observations and analysis

The observations were carried out in three observing runs at the Siding Spring Observatory, Australia. We took two-colour photometry and optical spectroscopy on six consecutive nights between June 28 and July 4, 2004 for V870 Ara, QY Hya, VZ Lib, and DX Tuc. Data for XY Leo were gathered on 4 nights in February, 2004 and 7 nights in March, 2005. The photometry was done using the 40-inch telescope of the Australian National University (ANU) in Siding Spring, equipped with the Imager CCD detector (2148×2048 pixels) and Johnson *B* and *V* filters. The exposure times ranged from 3 to 15 s, depending on the target brightness and weather conditions. For the optical spectroscopy, we used the ANU 2.3-m telescope and the Double Beam Spectrograph, recording the second order spectra of the 1200 mm^{-1} grating, which gave a nominal spectral resolution of $\lambda/\Delta\lambda \approx 7000$ at the $H\alpha$ line. We used only the red beam, covering $\sim 1000 \text{ \AA}$ between the sodium D doublet and the $H\alpha$ line.

All data were reduced in a standard fashion using IRAF¹. Photometric reductions included bias and flat-field correction, while instrumental magnitudes were determined with aperture photometry, because the stellar fields around the programme stars were quite empty, so that accurate psf-fitting was not possible. The instrumental data were tied to the standard system by observing equatorial photometric standard stars from the list of Landolt (1992), except for XY Leo, which was only observed under non-photometric conditions. The estimated uncertainty of the absolute values of the *B* and *V* magnitudes is about $\pm 0.01 \text{ mag}$.

¹ IRAF is distributed by the National Optical Astronomy Observatories, which are operated by the Association of Universities for Research in Astronomy, Inc., under cooperative agreement with the National Science Foundation.

Table 1. New times of primary (I) and secondary (II) minima for the target stars.

T_{\min} [HJD]	T_{\min} [HJD]	T_{\min} [HJD]
	XY Leo	
2 453 412.1839 II	2 453 415.0236 II	2 453 416.1621 II
2 453 413.0367 II	2 453 415.1671 I	2 453 435.0538 I
2 453 413.1793 I	2 453 416.0209 I	2 453 436.0479 II
	VZ Lib	
2 453 189.0102 II	2 453 190.9776 I	
	DX Tuc	
2 453 187.1669 II	2 453 188.2989 II	2 453 189.2421 I
	QY Hya	
2 453 186.9081 I	2 453 187.9276 II	
	V870 Ara	
2 453 185.1379 I	2 453 195.1314 I	2 453 196.1325 II

From the light curves we determined epochs of minimum light by fitting low-order polynomials. We measured 19 new times of minimum, which are collected in Table 1. The typical uncertainty is about $\pm 3 \times 10^{-4} \text{ d}$. With these we updated the O–C diagrams that were based on all published observations in the literature. For V870 Ara, QY Hya, and DX Tuc, we could derive a more accurate orbital period.

The spectra were also reduced with standard IRAF tasks, including bias and flat-field corrections, cosmic ray removal, extraction of one-dimensional spectra, wavelength calibration, and continuum normalization. The exposure times ranged from 2 to 5 min, and NeAr spectral lamp exposures were regularly taken to monitor the wavelength shifts of the CCD spectra. Radial velocities were determined by cross-correlation, with IAU radial velocity standards HD 187691 (F8V, $V_r = -0.2 \text{ km s}^{-1}$) and HD 80170 (K2III, $V_r = 0.5 \text{ km s}^{-1}$). The calculated cross-correlation functions (CCFs) were fitted with two- or three-component Gaussians (in case of detected tertiary components), whose centroids gave the radial velocities for each component. In most cases, the Gaussian approximation gave reasonably good fits for the central parts of the CCFs, while departures from the Gaussian shape typically occurred only 200–300 km s^{-1} away from the maxima.

The shape of the CCF clearly showed the presence of a tertiary component in three of the target stars. In those cases we recorded its mean radial velocity, which can be used in the future to detect orbital motion around the barycentre of the triple system. The binary radial velocity curves were fitted with sine curves, which gave the mean velocity of the binary (V_γ), the orbital velocities, and the mass ratio of the components (K_1 , K_2 , q). These were then used as fixed input parameters for the light curve models.

The rms scatter of the derived velocity data around sine-wave fits suggests that the typical velocity precision is about $\pm 10 \text{ km s}^{-1}$ per point. Although Rucinski (2002b) demonstrated that the use of the broadening function (BF) for determining the radial velocities of contact binaries is superior to the CCF method, we chose to apply the CCF for two reasons. First, IDL was not available to us so we could not use the BF codes². Second, the data have relatively poor spectral resolution and thus the CCF approach is sufficient. Nevertheless, besides estimating probable errors from the data, we also tested the accuracy of the velocity measurement method in the following way. First, a theoretical spectrum of a $T_{\text{eff}} = 5900 \text{ K}$, $\log g = 4.0$ star was

² <http://www.astro.utoronto.ca/~rucinski/SVDcookbook.html>

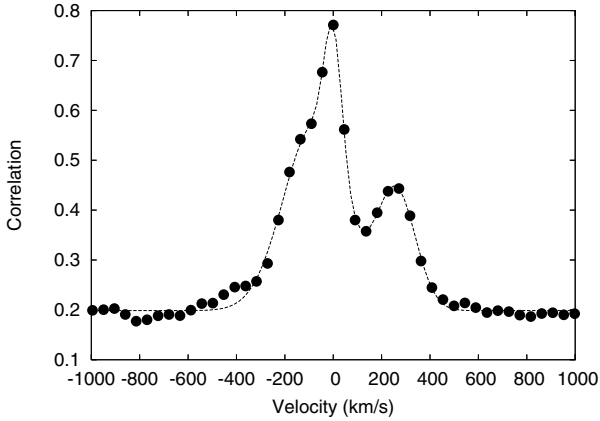


Fig. 1. A simulated CCF profile and the three-component Gaussian fit (see text for details).

calculated with Robert Kurucz’s ATLAS9 code between 5800 Å and 6800 Å and resampled to a resolution of ~ 8000 . Then, a contact binary broadening profile at quadrature phase ($\phi = 0.25$) was generated by Slavek Rucinski’s WUMA4 code, applying the physical parameters of VZ Lib, one of our programme stars (see Sect. 3.2). The model spectrum was then convolved with the broadening profile to get a contact binary model spectrum. A scaled original model spectrum (scaled to 20% of the initial flux level) at zero velocity was added to the contact binary model spectrum to mimic the presence of the tertiary component. This binary+tertiary spectrum was then cross-correlated with the original model spectrum. The resulting CCF, which is very similar to most of the real CCFs of our programme stars, is shown in Fig. 1.

The radial velocities were determined via fitting three-component Gaussians, as described above. The centroids recovered for the model spectrum are $a_1 = -80.5 \text{ km s}^{-1}$, $a_2 = 259.1 \text{ km s}^{-1}$ and $a_3 = 0.0 \text{ km s}^{-1}$, while the model velocities were initially $v_1 = -84 \text{ km s}^{-1}$, $v_2 = 252 \text{ km s}^{-1}$ and $v_3 = 0.0 \text{ km s}^{-1}$. It is seen that the error determining the velocity is within 10 km s^{-1} for the binary components and less than that (probably a few km s^{-1}) for the sharp-lined third component. These are clearly larger than the $1\text{--}2 \text{ km s}^{-1}$ error determined by Rucinski (2002b) for the BF-method, but our spectra have lower resolution than those applied by Rucinski (2002b). The numbers also show that the recovered velocities are shifted to the input values in the same direction, which means the effect is systematic, affecting both velocity amplitudes. We note that Rucinski and co-workers found that CCF tends to reduce the measured radial velocity amplitudes relative to the BF results (e.g. Rucinski 2004). Conservatively, we adopt a $\pm 8 \text{ km s}^{-1}$ error in the derived amplitudes K_1 and K_2 and $\pm 2 \text{ km s}^{-1}$ per point as the measurement uncertainty of the radial velocity of the tertiary component. These errors were added in quadrature to the formal errors of the calculated fits.

The light curves were modelled using the 2003 version³ of the Wilson-Devinney (WD) code (Wilson & Devinney 1971; Wilson 1994; Wilson & van Hamme 2003). Besides the spectroscopic parameters, we determined the effective temperature, T_1 , of the component eclipsed in zero phase from the $(B - V) - T_{\text{eff}}$ calibration of Gray (1992). The lower limit of the semimajor axis, A , was calculated from K_1 , K_2 , and P . These input parameters were kept fixed while running the WD code on the original individual data points. Limb-darkening coefficients

were taken from Diaz-Cordoves et al. (1995), while the bolometric albedos and gravity-darkening coefficients were set to 0.5 (Rucinski 1969) and 0.32 (Lucy 1967), respectively. The third light was included in the fitting procedure, except for DX Tuc and V870 Ara, for which we do not find evidence of a third component. In three cases, the brightness difference of the consecutive maxima (the O’Connell-effect, hereafter denoted by ΔV in the V band) suggested the presence of spots, which were added to the solution. The astrophysical coordinates of the centre of a given spot were fixed after several trials.

In cases of the multiple systems, we also estimated the physical parameters of the third bodies using the method described in Borkovits et al. (2002) and Csizmadia (2005). The light curve solutions yield the third light in different colours, and the colour index of the tertiary component follows from the colour index of the primary star as

$$(B - V)_3 = (B - V)_1 - 2.5 \left[\log \left(\frac{L_{3,B}}{L_{3,V}} \right) - \log \left(\frac{L_{1,B}}{L_{1,V}} \right) \right] \quad (1)$$

where $L_3 \approx 4\pi l_3$ (l_3 is the third light) and the luminosities are given in arbitrary units calculated by the WD-code. The colour index of the primary was estimated from the determined effective temperature using the temperature– $(B - V)$ relations by Flower (1996). With only two colours, we could not identify the location of the tertiary star in a two-colour diagram. Therefore, we assumed that the tertiary component is a main-sequence star. Then its spectral type can be estimated from the colour index using the Bessell (1990) tables, yielding an approximate mass estimate.

All the standardized light curves and radial velocity data are available electronically at the CDS.

3. Results

3.1. XY Leonis

XY Leo is a well-studied contact binary that has long been known for its cyclic period variations (Gehlich et al. 1972; Yakut et al. 2003). In stark contrast to the multitude of photometric studies (Yakut et al. 2003, and references therein), only two spectroscopic studies aimed at measuring radial velocity curves (Hrivnak et al. 1984; Barden 1987). XY Leo has four components. One pair is a W-type contact binary (i.e. the smaller star is the hotter one) with a very short orbital period ($P \approx 0.28 \text{ d}$) and late spectral type (Kn). It is a chromospherically active variable (Vilhu & Rucinski 1985), but the activity is largely dominated by the BY Dra-type binary component that consists of two red dwarf stars (Barden 1987).

Spectra taken in early 2004 showed a similar, though slightly weaker and unresolved $H\alpha$ emission than the one depicted in Fig. 1 of Barden (1987). The cross-correlation profiles of the spectra clearly indicated the presence of a third component (left panel in Fig. 2), so we fitted three Gaussians to measure radial velocities of the eclipsing pair (right panel in Fig. 2). The determined spectroscopic elements (Table 2) agree within the errorbars with the corresponding parameters from the literature (Barden 1987), except the γ -velocity. Since our observations were taken 19 years later than those of Barden (1987), which is close to the orbital period of the wide binary, this shift in V_γ might be due to the strong third light that distorts the whole CCF profile. Nevertheless, the agreement in the measured amplitudes suggests that the resulting velocity shift caused by the distorted CCF is very similar for both components.

The light curves (Fig. 3) do not show the O’Connell-effect, thus we did not include spots in the light curve fit. In this case

³ <ftp://ftp.astro.ufl.edu/pub/wilson>

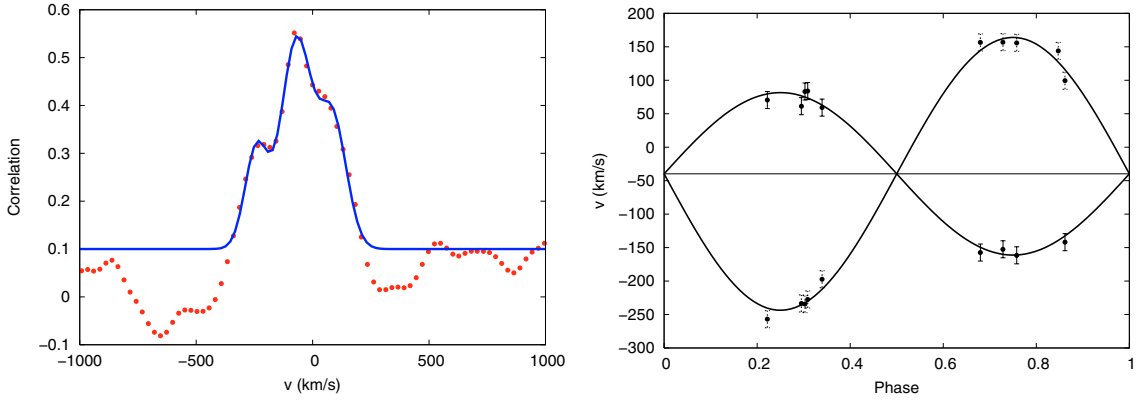


Fig. 2. *Left panel:* the CCF-profile of XY Leo in phase 0.75 with the three fitted Gaussians. *Right panel:* radial velocity curves of the eclipsing components of XY Leo.

Table 2. Physical parameters of XY Leo.

Parameter	This paper	Literature	Parameter	This paper	Literature
Spectroscopy					
$A \sin i [R_{\odot}]$	1.80 ± 0.11	1.84 ± 0.03	$K_1 [\text{km s}^{-1}]$	203.7 ± 9.1	204.7 ± 2.5
$V_{\gamma} [\text{km s}^{-1}]$	-36.7 ± 5.1	-51.8 ± 2.2	$K_2 [\text{km s}^{-1}]$	122.0 ± 10.0	124.1 ± 2.8
HJD ₃	2453456.5	–	$V_3 [\text{km s}^{-1}]$	-70.0 ± 7.5	–
Light curve fit					
$i [^{\circ}]$	67.1 ± 0.1	68 ± 1	Ω_1	4.7206 ± 0.0037	4.71 ± 0.01
f	5.2%	6.7%	Ω_2	4.7206	4.71
phase shift	0.0027 ± 0.0002	–	$(\frac{L_1}{L_1+L_2})_B$	0.553 ± 0.009	0.507 ± 0.043
q	$1.66(\pm 0.23)$	1.64	$(\frac{L_1}{L_1+L_2})_V$	0.522 ± 0.007	0.483 ± 0.043
$T_1 [\text{K}]$	4800	4850	$(l_3)_B$	0.051 ± 0.005	0.019 ± 0.007
$T_2 [\text{K}]$	4361 ± 8	4524 ± 14	$(l_3)_V$	0.068 ± 0.004	0.059 ± 0.007
$(B - V)_1$	1.02	–	$(B - V)_3$	2.02	–
Absolute parameters					
$M_1 [M_{\odot}]$	0.46 ± 0.06	0.50 ± 0.02	$M_2 [M_{\odot}]$	0.76 ± 0.15	0.82 ± 0.02
$R_1 [R_{\odot}]$	0.66 ± 0.10	0.68 ± 0.02	$R_2 [R_{\odot}]$	0.83 ± 0.13	0.85 ± 0.02
$L_1 [L_{\odot}]$	0.21 ± 0.07	0.226	$L_2 [L_{\odot}]$	0.22 ± 0.08	0.267
$(M_{\text{bol}})_1$	6.43 ± 0.23	6.4	$(M_{\text{bol}})_2$	6.34 ± 0.23	6.2
$(M_V)_1$	6.89 ± 0.23	6.7	$(M_V)_2$	6.96 ± 0.23	6.7
Sp. type (3)	M				
$d [\text{pc}]$	51 ± 6	63^{+8}_{-6}			

we had only differential light curves, so the fixed temperature of the primary component was estimated from the spectral type. The results (Table 2, where the values in italic denote fixed input parameters, while HJD₃ and V_3 refer to mean epoch and radial velocity of the third component – the same as by the next objects) are quite similar to the reference values (Yakut et al. 2003). The derived colour index of the third component is very red at $(B - V)_3 = 2.02$ mag, since consistent with a BY Dra-like M-dwarf binary (Barden 1987). For calculating the distance, we used the maximum V -brightness of the stars listed in ESA (1997).

With the most extended coverage of the period change, we also updated the O–C diagram. Since the publication of the Yakut et al. (2003) analysis, new moments of minima have been published by Agerer & Hübscher (2003), Drozd & Ogloza (2005), Hübscher (2005), Hübscher et al. (2005), and Nelson (2006). We also added a few epochs from Tsessevitch (1954a), which were not included in the analysis of Yakut et al. (2003) but were important in stretching the time coverage as far back as

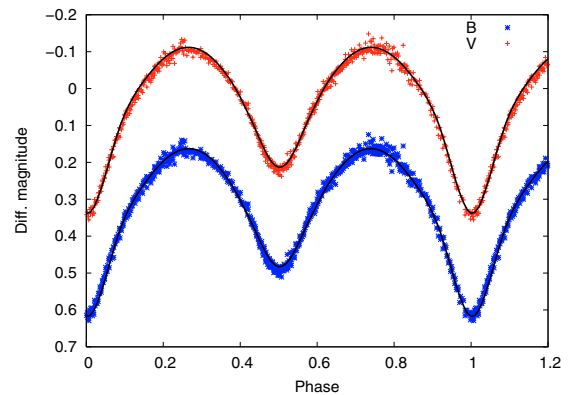


Fig. 3. Observed and fitted light curves of XY Leo.

possible. The full O–C diagram of XY Leo, plotted in the top panel of Fig. 4, was calculated using the ephemeris: $\text{HJD}_{\text{min}} = 2435484.0283 + 0.28410260 \times E$. Then we simultaneously

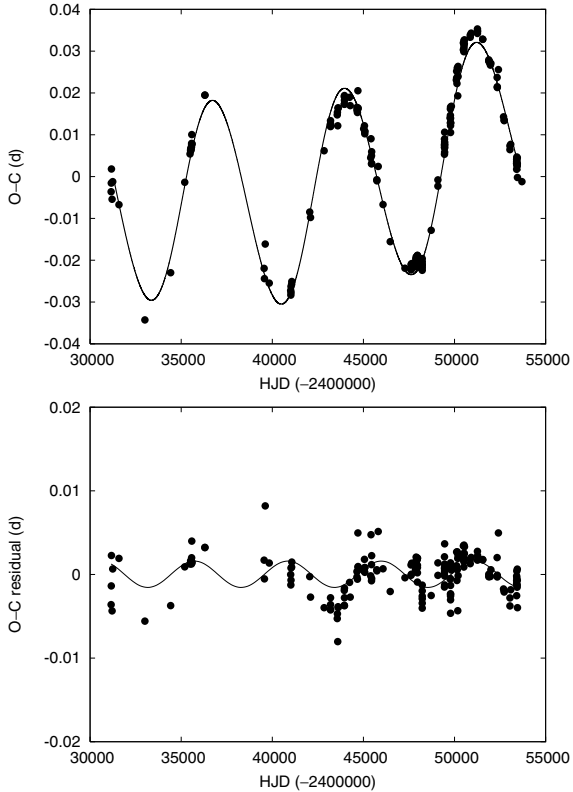


Fig. 4. *Top panel:* the O–C diagram of XY Leo with the theoretical fit. *Bottom panel:* the residuals and the ~ 5100 d secondary periodicity.

fitted a parabolic and a light-time term to calculate the rate of the linear period change and the orbital elements of the perturbing binary. For this, we used the same code as Ribas et al. (2002), kindly provided by Dr. I. Ribas.

The results are summarised in Table 3. In general, the parabolic term represents a continuous-period variation that might be explained by some mass transfer between the components. The period changing rate of XY Leo $\frac{1}{P} \frac{dP}{dt} = 2.85 \times 10^{-8} \text{ yr}^{-1}$, which can be translated into a mass-transfer rate of $-9.6 \times 10^{-9} M_{\odot}/\text{yr}$. This period variation rate is within the usual range of W UMa systems (see Qian 2001a,b; Borkovits et al. 2005 – XY Leo was not included in these studies). The secular orbital-period increase seems to support what Qian (2001a) suggests, namely that W-type systems with $q < 0.4$ and $q > 0.4$ tend to show secular decrease and increase, respectively.

The light-time parameters in Table 3 give very similar orbital elements for the quadruple system to all the previous investigations (Gehlich et al. 1972; Pan & Cao 1998; Yakut et al. 2003), so that we do not re-iterate the discussion of the hierarchic component. However, the residuals of the O–C fit deserve further discussion, because the 201 s rms is larger than the typical observational uncertainties. An analysis of the long-term period change of the triple W UMa VW Cep revealed secondary cycles in the O–C diagram that were interpreted as possible evidence of magnetic activity (Kaszás et al. 1998). More recently, Borkovits et al. (2005) investigated complex period variations of five W UMa-type binaries, finding some common features. These include secular period variation at a constant rate and a low-amplitude modulation with periods around 18–20 yr in four of the five cases. These stars all have spectral type later than F8 (so they have convective envelopes), while the fifth one is an A-type contact binary. XY Leo is a K-type star, therefore

Table 3. Parameters of the O–C fit, with the standard errors in the last digits shown in parentheses.

Parameter	value
A_{O-C} [d]	0.02430(1)
e	0.11(1)
ω [$^{\circ}$]	18.5(5)
P_3 [yr]	19.651(2)
$T_{\text{periastron}}$ [HJD]	2 446 119(11)
P_1 [d]	0.28410295(1)
dP/dt [s/d]	$1.92(6) \times 10^{-6}$

the secondary periodicity of the O–C diagram agrees with the picture suggested by Borkovits et al. (2005) that all contact binaries later than F8 have low-amplitude cyclic period changes. These can be interpreted as indirect evidence of magnetic cycles in late-type overcontact binaries that are analogous to the observed activity cycles in RS CVn systems (Hall 1989). The theoretical framework involves the interchange of magnetic and kinetic energy (Applegate 1992; Lanza & Rodonò 2002), predicting time scales from several years to decades.

The bottom panel of Fig. 4 shows the best-fit sine wave to the residuals of the O–C. Introducing this extra component decreases the rms to ~ 175 s, which represents a slight but detectable improvement and agrees with the typical photometric noise from starspots (Kalimeris et al. 2002). The Fourier spectrum of the residuals shows that the highest peak has an S/N ratio (Breger et al. 1993) of 3, thus its significance is marginal. Nevertheless, the corresponding modulation period (~ 5100 d or 14 yr) and amplitude (0.0016 d) are very similar to those found by Borkovits et al. (2005) for AB And, OO Aql, V566 Oph and U Peg. We therefore conclude that XY Leo is likely to bear signatures of short-period magnetic cycles in W UMa-type variables, but several years of further continuous eclipse timings are needed to improve the significance of the detection.

3.2. VZ Librae

The variability of the F5-type star VZ Lib was discovered by Hoffmeister (1933), who gave neither period nor classification but recognised its low-amplitude eclipsing nature. Tsessevich (1954b) classified the star as a W UMa-type variable with a period slightly over 8 h. Claria & Lapasset (1981) reported the first photoelectric light curve that showed a difference in the eclipse depths for the primary and the secondary minima of about 0.1 mag. Interestingly, more recent observations, including ours and those of Zola et al. (2004), find more similar minima with differences of only 0.02–0.03 mag (Zola et al. 2004) and < 0.01 mag (this paper) in V . There is a relatively bright tertiary component in the system discovered by Lu et al. (2001). Besides finding radial velocity variations of the third star up to 40 km s^{-1} over a period of 1200 days, they derived a luminosity ratio of $L_3/L_{12} = 0.20 \pm 0.04$. In contrast Zola et al. (2004) arrived at only a few percent (4–5) of third light contribution, which was left unexplained.

The cross-correlation profiles of our spectra clearly indicated the presence of a third, narrow-lined companion (left panel in Fig. 5). Its mean radial velocity is $-4.8 \pm 3 \text{ km s}^{-1}$, which is higher than any of the velocities in Fig. 5 of Lu et al. (2001), ranging from -9 to -50 km s^{-1} . Apart from pushing up the full velocity range of the third component well over 40 km s^{-1} , this value strongly suggests that the 1200 d of observations

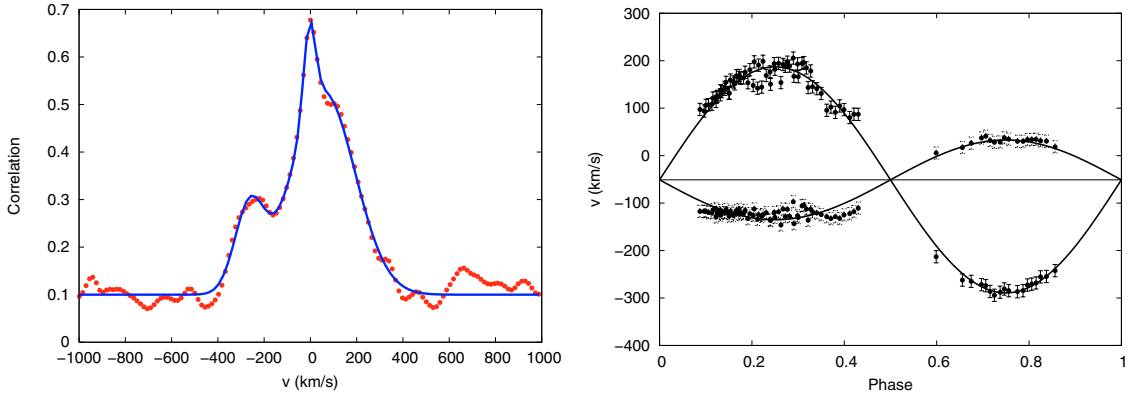


Fig. 5. *Left panel:* the CCF-profile of VZ Lib in phase 0.75 with the three fitted Gaussians. *Right panel:* radial velocity curves of the eclipsing components of VZ Lib.

Table 4. Physical parameters of VZ Lib.

Parameter	This paper	Literature	Parameter	This paper	Literature
Spectroscopy					
$A \sin i [R_{\odot}]$	2.38 ± 0.12	2.53 ± 0.06	$K_1 [\text{km s}^{-1}]$	84.1 ± 8.2	68.5 ± 3.8
$V_{\gamma} [\text{km s}^{-1}]$	-51.1 ± 1.9	-31.1 ± 2.3	$K_2 [\text{km s}^{-1}]$	252.2 ± 8.3	289.2 ± 4.6
HJD ₃	2453189.4	–	$V_3 [\text{km s}^{-1}]$	-4.8 ± 3	–
Light curve fit					
$i [^{\circ}]$	88.4 ± 1.0	80.3 ± 0.5	r_1^{side}	0.4908 ± 0.0009	0.5122 ± 0.0012
phase shift	-0.0004 ± 0.0003	-0.0030 ± 0.0004	r_2^{side}	0.2905 ± 0.0008	0.2655 ± 0.0011
q	$0.33(\pm 0.04)$	0.255	r_1^{back}	0.5195 ± 0.0011	0.5378 ± 0.0015
$T_1 [\text{K}]$	5770	5920	r_2^{back}	0.3303 ± 0.0014	0.3022 ± 0.0020
$T_2 [\text{K}]$	5980 ± 12	6030 ± 21	f	19.4%	13%
Ω_1	2.498 ± 0.003	2.344 ± 0.004	$(\frac{L_1}{L_1+L_2})_B$	0.686 ± 0.002	0.757 ± 0.001
Ω_2	2.498	2.344	$(\frac{L_1}{L_1+L_2})_V$	0.545 ± 0.009	0.759 ± 0.002
r_1^{pole}	0.4558 ± 0.0007	0.4732 ± 0.0009	$l_3 (B)$	0.192 ± 0.007	0.011 ± 0.005
r_2^{pole}	0.2777 ± 0.0007	0.2545 ± 0.0010	$l_3 (V)$	0.209 ± 0.004	0.043 ± 0.009
$(B - V)_1$	0.63	–	$(B - V)_3$	0.73	–
Absolute parameters					
$M_1 [M_{\odot}]$	1.06 ± 0.06	1.480 ± 0.068	$M_2 [M_{\odot}]$	0.35 ± 0.03	0.378 ± 0.034
$R_1 [R_{\odot}]$	1.17 ± 0.05	1.34 ± 0.02	$R_2 [R_{\odot}]$	0.72 ± 0.03	0.69 ± 0.01
$L_1 [L_{\odot}]$	1.36 ± 0.19	–	$L_2 [L_{\odot}]$	0.59 ± 0.05	–
$(M_{\text{bol}})_1$	4.39 ± 0.11	–	$(M_{\text{bol}})_2$	5.29 ± 0.11	–
$(M_V)_1$	4.60 ± 0.11	–	$(M_V)_2$	5.48 ± 0.11	–
Sp. type (3)	G7	–	$M_3 [M_{\odot}]$	0.90	–
$d [\text{pc}]$	171 ± 8	–			

by Lu et al. (2001) was shorter than the orbital period of the third component.

The radial velocity curve (right panel in Fig. 5) yields a higher mass ratio than that of Lu et al. (2001), but it is still compatible with the earlier result of $q = 0.24 \pm 0.07$ that was based on a relatively poor radial velocity solution. The light curves (Fig. 6) are very similar to those of Zola et al. (2004), except that the O’Connell-effect was not detectable in 2004. Consequently, our light curve fit did not include spots on any of the components.

A comparison of the determined parameters with the published ones (Lu et al. 2001 – spectroscopy; Zola et al. 2004 – light curve fit and absolute parameters) shows relatively good agreement (Table 4). The differences can largely be traced back to our higher mass ratio and the different amount of the third light. The strong tertiary peak in the CCF-profile supports the $\sim 20\%$ luminosity contribution of the third component, which is also close to the value determined by Lu et al. (2001). Since the Zola et al. light curve model is not consistent with this, we are confident that our light curve solution is more compatible with

the available spectroscopic information. To remove most of the ambiguities, a better defined radial velocity curve is highly desirable, preferentially from higher-resolution and S/N spectra.

Because the tertiary component is comparable in luminosity (and perhaps in mass) to the eclipsing pair, one can expect a measurable light-time effect in the period change. Since the study of Claria & Lapasset (1981) of only the Hipparcos photometry, Zola et al. (2004) and Krajci (2006) presented new epochs of minimum light, which is hardly enough to reconstruct the hypothetic cyclic period changes. On the other hand, the ASAS-3 project (Pojmanski 2002) has been observing this system since 2001 and produced 259 V-band points scattered between JD 2451918–2453277. We combined the recent data as follows.

First we adopted the linear ephemeris of Zola et al. (2004): $E_0 = 2452727.4047$, $P = 0.3582580$ d. Then we cut the ASAS data into 4 equal subsets, which correspond to four observing seasons since the beginning of the project. We phased all the subsets using the given ephemeris, and the resulting phase diagrams yielded the phase-shifts of the primary minimum.

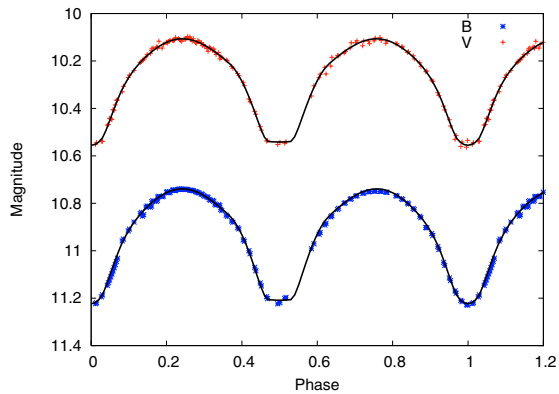


Fig. 6. Observed and fitted light curves of VZ Lib.

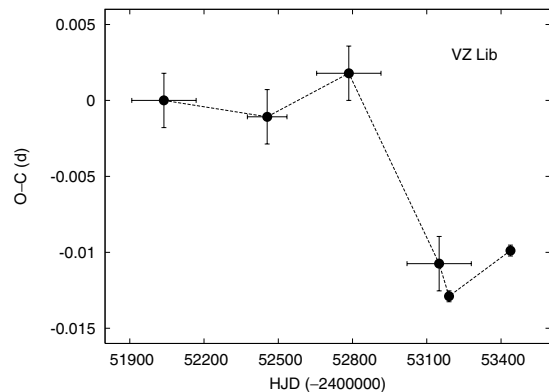


Fig. 7. The O–C diagram of VZ Lib between 2000–2006 (see text for details).

In Fig. 7 we plot the results (multiplied by the period), where the last two points were calculated from our primary minimum and that of Krajci (2006).

The shape of the O–C diagram indicates measurable phase changes over the past 6 years. This may be interpreted as possible evidence of period variations due to light-time effect in the triple system, although other mechanisms, like magnetic activity or sudden mass exchange via large flares, cannot be ruled out either. Assuming a light-time effect, both the long-term radial velocity curve (Lu et al. 2001) and Fig. 7 suggest that the orbital period of the third component is longer than 1200–1500 d. Regular future eclipse timings will therefore be crucial in sorting out different mechanisms of period change and, ultimately, improving our understanding of the system.

3.3. DX Tucanae

The variability of DX Tuc was discovered by the Hipparcos satellite, and it was classified as an F7-type contact binary (ESA 1997; Kazarovets et al. 1999). Pribulla et al. (2003) listed the star in their catalog of field contact binary stars. Selam (2004), based on the Fourier-decomposition of the Hipparcos light curve, put it among the 64 genuine W UMa-type variables, while Pribulla & Rucinski (2006) did not find any indication of multiplicity (caused mainly by the lack of available data in the literature).

The radial velocity curve and standard photometry presented here (Figs. 8–9) are the first ones in the literature. Using the Hipparcos ephemeris ($HJD_{\min} = 2\,448\,500.2540$) and the new times of minimum light, we calculated an improved orbital period $P_{\text{orb}} = 0.37711010(2)$ d.

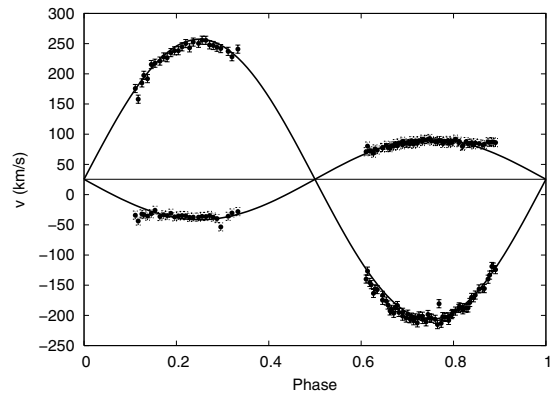


Fig. 8. Radial velocity curve of DX Tuc.

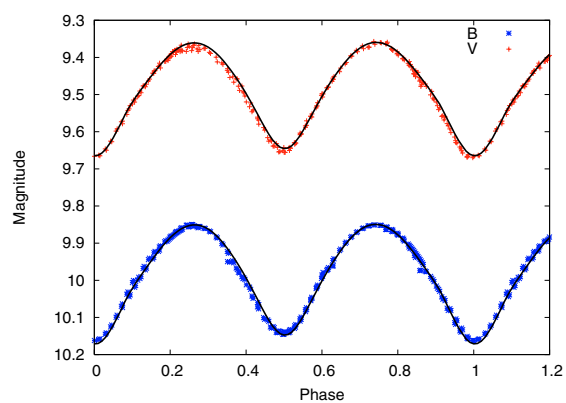


Fig. 9. Observed and fitted light curves of DX Tuc.

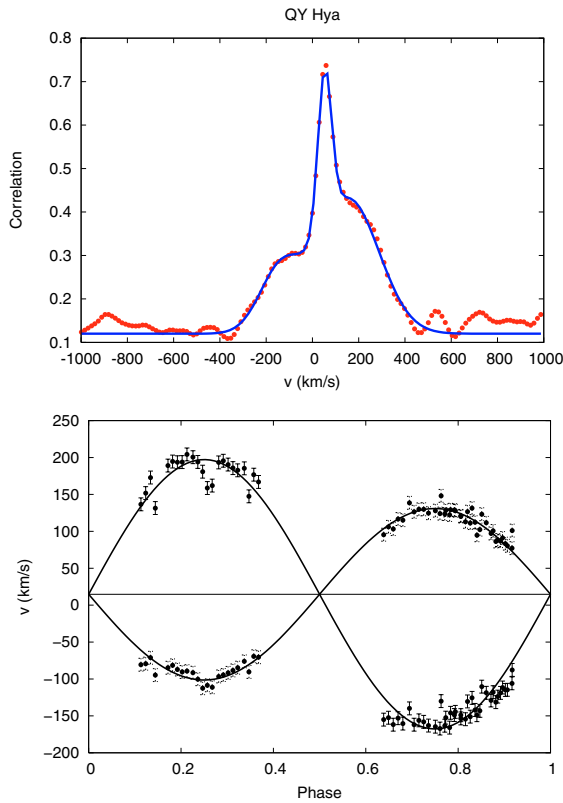
The full set of physical parameters is given in Table 5. The system is a typical contact binary, which has two components of very different masses but similar temperatures. Nevertheless, the larger star is slightly hotter, which puts DX Tuc among the A-type W UMa systems. The light curve shows a small but detectable O’Connell-effect ($\Delta V = 0.01$ mag), so we included a spot in the light curve model. With no indication of a third component in the cross-correlation profile, we fixed $l_3 = 0$. For calculating the absolute parameters, we assumed zero interstellar reddening, which is supported by the reddening map of Schlegel et al. (1998) that implies $E(B - V) \leq 0.017$ mag in this direction.

3.4. QY Hydrae

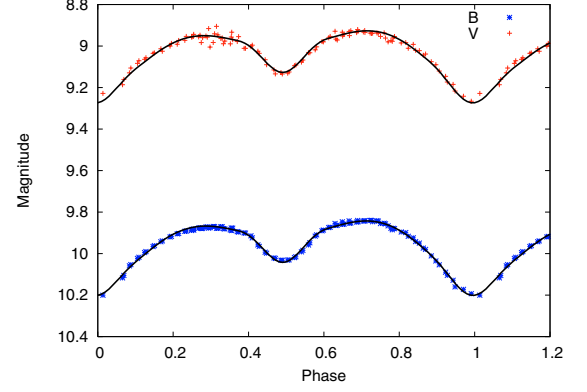
The variability of QY Hydrae was discovered by the Hipparcos satellite (ESA 1997) and the variable star designation was given by Kazarovets et al. (1999). Although it belongs to the 100 brightest X-ray stars within 50 parsecs of the Sun (Makarov 2003), no detailed study has been done so far. (We note that Makarov (2003) listed the star erroneously as QY Lyr.) The late spectral type (K2V) and the short orbital period put QY Hya in the XO class of X-ray active stars by Makarov (2003), whose group includes binary stars of BY Dra-type, detached binaries (Algols), and eclipsing binaries of β Lyr type. Selam (2004) clearly separates QY Hya from the W UMa stars using the Fourier-description of the Hipparcos light curve, confirming the β Lyr class. There is one measurement of the radial velocity, $+25.4 \pm 0.6$ km s $^{-1}$, published by Nordström et al. (2004). They observed the star among $\sim 14\,000$ F and G dwarfs, thus avoiding the detection of possible time variability of the radial velocity.

Table 5. Physical parameters of DX Tuc.

Parameter	Value	Parameter	Value
Spectroscopy			
$A \sin i [R_\odot]$	2.24 ± 0.12	$K_1 [\text{km s}^{-1}]$	66.8 ± 8.1
$V_\gamma [\text{km s}^{-1}]$	25.4 ± 0.8	$K_2 [\text{km s}^{-1}]$	233.8 ± 8.1
Light curve fit			
$i [^\circ]$	62.3 ± 0.2	r_1^{side}	0.5059 ± 0.0006
phase shift	0.0022 ± 0.0002	r_2^{side}	0.2850 ± 0.0006
q	$0.29(\pm 0.04)$	r_1^{back}	0.5348 ± 0.0008
$T_1 [\text{K}]$	6250	r_2^{back}	0.3279 ± 0.0010
$T_2 [\text{K}]$	6182 ± 37	f^2	14.9%
Ω_1	2.408 ± 0.002	$(\frac{L_1}{L_1+L_2})_B$	0.756 ± 0.002
Ω_2	2.408	$(\frac{L_1}{L_1+L_2})_V$	0.755 ± 0.001
r_1^{pole}	0.4676 ± 0.0004	$l_3 (B)$	0.0
r_2^{pole}	0.2721 ± 0.0005	$l_3 (V)$	0.0
Spot parameters			
Co-lat. [deg]	92	Rad. [deg]	26
Long. [deg]	175	T_{fact}	0.97 ± 0.01
Absolute parameters			
$M_1 [M_\odot]$	1.00 ± 0.03	$M_2 [M_\odot]$	0.30 ± 0.01
$R_1 [R_\odot]$	1.20 ± 0.04	$R_2 [R_\odot]$	0.71 ± 0.02
$L_1 [L_\odot]$	1.97 ± 0.25	$L_2 [L_\odot]$	0.66 ± 0.04
$(M_{\text{bol}})_1$	3.98 ± 0.10	$(M_{\text{bol}})_2$	5.17 ± 0.10
$(M_V)_1$	4.13 ± 0.10	$(M_V)_2$	5.34 ± 0.10
$d [\text{pc}]$	128 ± 6		

**Fig. 10.** Top panel: the CCF-profile of QY Hya in phase 0.75 with the three Gaussian components. Bottom panel: radial velocities of the eclipsing components of QY Hya.

We obtained standard BV light curves with full phase coverage and an excellent coverage of the radial velocity curve (Figs. 10–11). The cross-correlation profile shows the presence of a third light at $V_3 \approx +50 \text{ km s}^{-1}$ (top panel in Fig. 10). Using the Hipparcos ephemeris ($\text{HJD}_{\text{min}} = 2448\,500.2490$) and our

**Fig. 11.** Observed and fitted light curves of QY Hya.**Table 6.** Physical parameters of QY Hya.

Parameter	Value	Parameter	Value
Spectroscopy			
$A \sin i [R_\odot]$	1.68 ± 0.10	$K_1 [\text{km s}^{-1}]$	117.0 ± 8.1
$V_\gamma [\text{km s}^{-1}]$	14.8 ± 1.6	$K_2 [\text{km s}^{-1}]$	178.1 ± 8.4
HJD ₃	2453186.4	$V_3 [\text{km s}^{-1}]$	53.1 ± 2.4
Light curve fit			
$i [^\circ]$	63.1 ± 0.6	r_1^{side}	0.4128 ± 0.0034
phase shift	-0.009 ± 0.001	r_2^{side}	0.3079 ± 0.0034
q	$0.66(\pm 0.07)$	r_1^{back}	0.4421 ± 0.0048
$T_1 [\text{K}]$	5030	r_2^{back}	0.3287 ± 0.0048
$T_2 [\text{K}]$	5270 ± 84	f^2	—
Ω_1	<u>3.177</u>	$(\frac{L_1}{L_1+L_2})_B$	0.552 ± 0.012
Ω_2	3.357 ± 0.044	$(\frac{L_1}{L_1+L_2})_V$	0.569 ± 0.010
r_1^{pole}	0.3907 ± 0.0028	$l_3 (B)$	0.207 ± 0.077
r_2^{pole}	0.2974 ± 0.0028	$l_3 (V)$	0.154 ± 0.041
$(B - V)_1$	0.91	$(B - V)_3$	0.63
Spot parameters			
Co-lat. [deg]	33	Rad. [deg]	46
Long. [deg]	350	T_{fact}	0.84 ± 0.01
Absolute parameters			
$M_1 [M_\odot]$	0.667 ± 0.014	$M_2 [M_\odot]$	0.442 ± 0.017
$R_1 [R_\odot]$	0.80 ± 0.03	$R_2 [R_\odot]$	0.60 ± 0.03
$L_1 [L_\odot]$	0.37 ± 0.06	$L_2 [L_\odot]$	0.25 ± 0.01
$(M_{\text{bol}})_1$	5.80 ± 0.13	$(M_{\text{bol}})_2$	6.23 ± 0.13
$(M_V)_1$	6.24 ± 0.13	$(M_V)_2$	6.51 ± 0.13
Sp. type (3)	G4	$M_3 [M_\odot]$	0.97
$d [\text{pc}]$	50 ± 2		

new epochs of minimum light, we determined an updated mean period of $P_{\text{orb}} = 0.29234050(8) \text{ d}$.

The light curve fit indicates a semi-detached binary of similar components (Table 6; underlined values were calculated and fixed by the WD-code). There is a slight but significant brightness difference of $\Delta V = 0.035 \text{ mag}$ between the two maxima, which can be explained by a dark spot on the primary component. The calculated absolute parameters are based on the assumption of negligible interstellar reddening (the reddening map of Schlegel et al. (1998) gives an upper limit of $E(B - V) \leq 0.07 \text{ mag}$ towards QY Hya, so the $\sim 50 \text{ pc}$ distance to the star indeed implies a small colour excess). The third light seems to have similar contributions in B and V , like the third star in VZ Lib, which suggests a hierarchic triple system of three similar components.

Table 7. Physical parameters of V870 Ara.

Parameter	Value	Parameter	Value
Spectroscopy			
$A \sin i [R_{\odot}]$	2.43 ± 0.13	$K_1 [\text{km s}^{-1}]$	23.3 ± 8
$V_{\gamma} [\text{km s}^{-1}]$	11.5 ± 0.8	$K_2 [\text{km s}^{-1}]$	283.5 ± 8.1
Light curve			
$i [^{\circ}]$	70.0 ± 0.5	r_1^{side}	0.6424 ± 0.0007
phase shift	0.0023 ± 0.0005	r_2^{side}	0.2109 ± 0.0007
q	$0.082(\pm 0.030)$	r_1^{back}	0.6634 ± 0.0008
$T_1 [\text{K}]$	5860	r_2^{back}	0.3033 ± 0.0081
$T_2 [\text{K}]$	6210 ± 35	f	96.4%
Ω_1	1.849 ± 0.001	$(\frac{L_1}{L_1+L_2})_B$	0.852 ± 0.001
Ω_2	1.849	$(\frac{L_1}{L_1+L_2})_V$	0.860 ± 0.001
r_1^{pole}	0.5653 ± 0.0004	$l_3 (B)$	0.0
r_2^{pole}	0.1996 ± 0.0005	$l_3 (V)$	0.0
Spot parameters			
Co-lat. 1 [deg]	90	Rad. 1 [deg]	17
Long. 1 [deg]	84	$T_{\text{fact}} 1$	0.90 ± 0.01
Co-lat. 2 [deg]	57	Rad. 2 [deg]	26
Long. 2 [deg]	0	$T_{\text{fact}} 2$	0.94 ± 0.01
Absolute parameters			
$M_1 [M_{\odot}]$	1.503 ± 0.011	$M_2 [M_{\odot}]$	0.123 ± 0.002
$R_1 [R_{\odot}]$	1.67 ± 0.01	$R_2 [R_{\odot}]$	0.61 ± 0.01
$L_1 [L_{\odot}]$	2.96 ± 0.30	$L_2 [L_{\odot}]$	0.50 ± 0.01
$(M_{\text{bol}})_1$	3.54 ± 0.10	$(M_{\text{bol}})_2$	5.48 ± 0.10
$(M_V)_1$	3.74 ± 0.10	$(M_V)_2$	5.65 ± 0.10
$d [\text{pc}]$	107 ± 5		

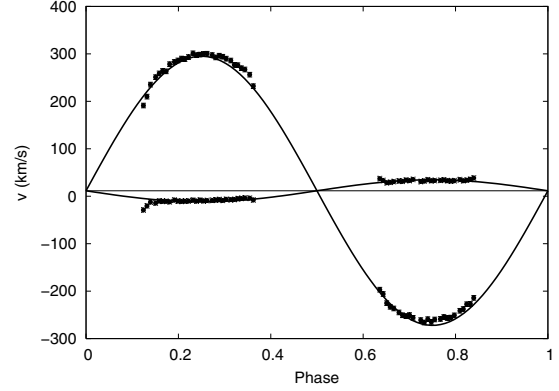
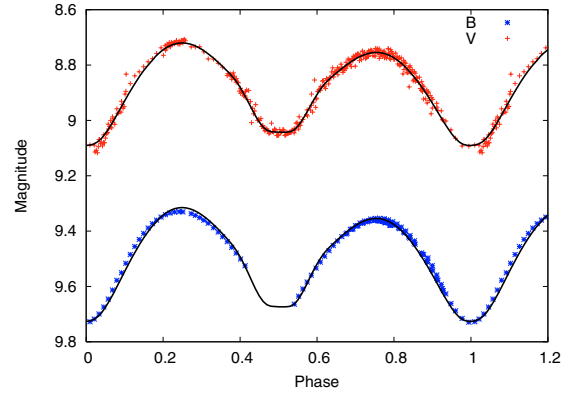
3.5. V870 Arae

V870 Ara is another Hipparcos discovery, classified as an F8-type contact binary (ESA 1997; Kazarovets et al. 1999). Pribulla et al. (2003) listed the star in their catalog of field contact binary stars. Selam (2004), based on the Fourier-decomposition of the Hipparcos light curve, put it among the 64 genuine W UMa-type variables, while Pribulla & Rucinski (2006) did not find any indication of multiplicity (caused largely by the lack of data in the literature).

The radial velocity curve and standard photometry presented here (Figs. 12–13) are the first ones in the literature. Using the Hipparcos ephemeris ($\text{HJD}_{\text{min}} = 2\,448\,500.1840$) and the new times of minimum light, we calculated an improved orbital period $P_{\text{orb}} = 0.39972200(2)$ d.

The most interesting feature about V870 Ara is the very small mass ratio $q = 0.082 \pm 0.030$. There are only two contact binaries with spectroscopically measured mass ratios around or below 0.08: AW UMa ($q \approx 0.075$, Rucinski 1992), SX Crv ($q \approx 0.066$, Rucinski et al. 2001); and one star, V857 Her, for which the best-fit light curve solutions strongly suggest a mass ratio somewhat less than 0.07 but lacking spectroscopic confirmation (Qian et al. 2005). The existence of these stars is important, because theory currently predicts a cutoff at about $q = 0.09$ (Rasio 1995), which might be pushed a bit lower to $q = 0.076$ (Li & Zhang 2006). Below that, contact binaries are expected to merge into a single fast-rotating star within 10^3 – 10^4 yrs. This puts V870 Ara among the objects that have the potential of constraining the evolutionary scenarios of binary mergers.

Because of the well-expressed O’Connell-effect ($\Delta V = 0.032$ mag) and asymmetric distortions of the light curve, we added two spots to the light curve solution. They rather represent the difficulties we met during the light curve modelling than two real compact features on the hot component. The finally adopted

**Fig. 12.** Radial velocity curve of V870 Ara.**Fig. 13.** Observed and fitted light curves of V870 Ara.

set of parameters (Table 7) shows, that despite its extreme mass ratio, this is a typical W-type W UMa system.

4. Summary

In this paper we have presented new photometric and spectroscopic data and their basic analysis for five close eclipsing binary stars. The sample consisted of three southern and two equatorial variables, of which the southern objects have never been observed and modelled since their discovery. The main results of this investigation can be summarised as follows:

- XY Leo is a hierarchic quadruple system with a W UMa-type contact binary and a BY Dra-type red dwarf binary. It is one of the best cases for the light-time effect in a periodic variable star. Besides determining new spectroscopic elements and a light curve solution, we also found weak evidence of short-period magnetic cycles.
- VZ Lib is another multiple system in which we detect the third component both spectroscopically and photometrically. Recent data indicate the possibility of a detectable light-time effect, thus further eclipse timings are needed to measure the orbital period of the tertiary companion.
- DX Tuc is a typical A-type W UMa star (i.e. the larger component is hotter).
- As one of the 100 brightest X-ray active stars within 50 parsecs of the Sun, QY Hya is a late-type triple system with a semi-detached eclipsing pair.
- Finally, V870 Ara is a contact binary with the third smallest spectroscopic mass ratio in all W UMa stars to date.

The consistency of the presented results can be tested with the Hipparcos distances. A comparison of the calculated distances

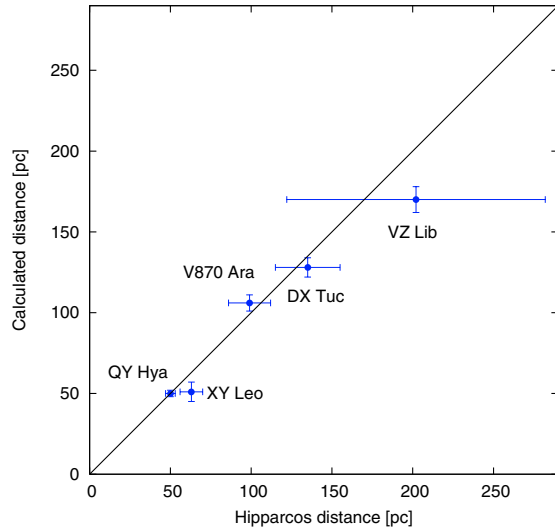


Fig. 14. A comparison of the calculated distances with the Hipparcos measurements.

that are based on the light curve models and the parallax-based Hipparcos values show good agreement for all the programme stars (Fig. 14). In the cases of DX Tuc and VZ Lib, the distances from light curve models are likely to be improvements over the Hipparcos values. We note that both the two most deviant stars, XY Leo and VZ Lib, have bright tertiary components, which may have introduced a systematic error into the Hipparcos astrometry that can explain the greater disagreement.

Acknowledgements. This work was supported by a University of Sydney Postdoctoral Research Fellowship, the Australian Research Council, and the Hungarian OTKA Grants #T042509 and #TS049872. We thank A. Derekas for assisting with the photometric observations in Siding Spring, Australia.

References

- Agerer, F., & Hübscher, J. 2003, IBVS, No. 5484
 Applegate, J. H. 1992, ApJ, 385, 621
 Barden, S. C. 1987, ApJ, 317, 333
 Bessell, M. S. 1990, PASP, 102, 1181
 Bilir, S., Karatas, Y., Demircan, O., & Eker, Z. 2005, MNRAS, 357, 497
 Borkovits, T., Csizmadia, Sz., Hegedüs, T., et al. 2002, A&A, 392, 895
 Borkovits, T., Elkhateeb, M. M., Csizmadia, Sz., et al. 2005, A&A, 441, 1087
 Breger, M., Stich, J., Garrido, R., et al. 1993, A&A, 271, 482
 Chen, W. P., Sanchawala, K., & Chiu, M. C. 2006, AJ, 131, 990
 Claria, J. J., & Lapasset, E. 1981, IBVS, No. 2035
 Csizmadia, Sz. 2005, Ph.D. Thesis, Eötvös University, Dept. of Astronomy, Budapest
 Csizmadia, Sz., & Klagyivik, P. 2004, A&A, 426, 1001
 D'Angelo, C., van Kerkwijk, M. H., & Rucinski, S. M. 2006, AJ, 132, 650
 Diaz-Cordoves, J., Claret, A., & Gimenez, A. 1995, A&AS, 110, 329
 Drozd, M., & Ogloza, W. 2005, IBVS, No. 5623
 Duerbeck, H. W., & Rucinski, S. M. 2007, AJ, 133, 169
 Eggleton, P. 2006, Evolutionary processes in Binary and Multiple Stars (Cambridge University Press)
 Eggleton, P., & Kiseleva-Eggleton, L. 2001, ApJ, 562, 1012
 ESA 1997, The Hipparcos and Tycho Catalogues, ESA SP-1200
 Flower, P. J. 1996, ApJ, 469, 355
 Gehlich, U. K., Prolls, J., & Wehmeyer, R. 1972, A&A, 18, 477
 Geske, M. T., Gettel, S. J., & McKay, T. A. 2006, AJ, 131, 633
 Gray, F. 1992, The Observation and Analysis of Stellar Photospheres (Cambridge University Press)
 Hall, D. S. 1989, Space Sci. Rev., 50, 219
 Hoffmeister, C. 1933, AN, 247, 281
 Hrivnak, B. J., Milone, E. F., Hill, G., & Fisher, W. A. 1984, ApJ, 285, 683
 Hübscher, J. 2005, IBVS, No. 5643
 Hübscher, J., Paschke, A., & Walter, F. 2005, IBVS, No. 5657
 Kalimeris, A., Rovithis-Livaniou, H., & Rovithis, P. 2002, A&A, 387, 969
 Kaszás, G., Vinkó, J., Szatmáry, K., et al. 1998, A&A, 331, 231
 Kazarovets, A. V., Samus, N. N., Durlevich, O. V., et al. 1999, IBVS, No. 4659
 Krajci, T. 2006, IBVS, No. 5690
 Kreiner, J. M., Rucinski, S. M., Zola, S., et al. 2003, A&A, 412, 465
 Landolt, A. U. 1992, AJ, 104, 340
 Lanza, A. F., & Rodonò, M. 1999, A&A, 439, 887
 Lanza, A. F., & Rodonò, M. 2002, AN, 323, 424
 Li, L., & Zhang, F. 2006, MNRAS, 369, 2001
 Lu, W., Rucinski, S. M., & Ogloza, W. 2001, AJ, 122, 402
 Lucy, L. B. 1967, Z. Astrophys., 65, 89
 Maceroni, C., & van't Veer, F. 1996, A&A, 311, 523
 Makarov, V. V. 2003, AJ, 126, 1996
 Mochnacki, S. 1981, ApJ, 245, 650
 Nelson, R. H. 2006, IBVS, No. 5672
 Nordstrom, B., Mayor, M., Andersen, J., et al. 2004, A&A, 418, 989
 Pan, L., & Cao, M. 1998, Ap&SS, 259, 285
 Pojmanski, G. 2002, AcA, 52, 397
 Pribulla, T., & Rucinski, S. M. 2006, AJ, 131, 2986
 Pribulla, T., Kreiner, J. M., & Tremko, J. 2003, Comm. Skalnaté Pleso Obs., 33, 38
 Qian, S. B. 2001a, MNRAS, 328, 635
 Qian, S. B. 2001b, MNRAS, 328, 914
 Qian, S. B., Zhu, L.-Y., Soonthornthum, B., et al. 2005, AJ, 130, 1206
 Rasio, F. A. 1995, ApJ, 444, L41
 Ribas, I., Arenou, F., & Guinan, E. F. 2002, AJ, 123, 2033
 Rucinski, S. M. 1969, AcA, 19, 245
 Rucinski, S. M. 1992, AJ, 104, 1968
 Rucinski, S. M. 2002a, PASP, 114, 1124
 Rucinski, S. M. 2002b, AJ, 124, 1746
 Rucinski, S. M. 2004, Stellar rotation, ed. A. Maeder, & P. Eenens, Proc. IAU Symp. 215, 17
 Rucinski, S. M., & Duerbeck, H. W. 1997, PASP, 109, 1340
 Rucinski, S. M., & Duerbeck, H. W. 2006, AJ, 132, 1539
 Rucinski, S. M., Lu, W., Mochnacki, S. W., Ogloza, W., & Stachowski, G. 2001, AJ, 122, 1974
 Schlegel, D. J., Finkbeiner, D. P., & Davis, M. 1998, ApJ, 500, 525
 Selam, S. O. 2004, A&A, 416, 1097
 Stepień, K. 1995, MNRAS, 274, 1019
 Stepień, K., Schmitt, J. H. M. M., & Voges, W. 2001, A&A, 370, 157
 Tsessevich, V. P. 1954a, Izv. Astr. Obs. Odessa, 4, 179
 Tsessevich, V. P. 1954b, Izv. Astr. Obs. Odessa, 4, 196
 Vilhu, O., & Rucinski, S. M. 1985, AcA, 35, 29
 Wilson, R. E. 1994, PASP, 106, 921
 Wilson, R. E., & Devinney, E. J. 1971, ApJ, 166, 605
 Wilson, R. E., & van Hamme, W. 2003, Computing Binary Stars Observables, Ver. 4 (Gainesville: Univ. Florida)
 Yakut, K., Ibanoglu, C., Kalomeni, B., & Degirmenci, Ö. L. 2003, A&A, 401, 1095
 Zola, S., Rucinski, S. M., Baran, A., et al. 2004, AcA, 54, 299